

A POD based non-linear observer for unsteady flows

Edoardo Lombardi

MAB - Université Bordeaux I, France

Jessie Weller

MAB - Université Bordeaux I, France

Marcelo Buffoni

AFM - University of Southampton, UK

Angelo Iollo

MAB - Université Bordeaux I and INRIA Project MC2, France

Summary

1. Motivation
2. Low-dimensional modeling of unsteady flows
 - (a) Low-order model construction
 - (b) Low-order model with feedback control construction
3. A non-linear state observer for unsteady flows
 - (a) Non-linear observer
 - (b) Results
 - i. Two-dimensional case with feedback control: $Re = 150$
 - ii. Three-dimensional case: $Re = 300$
4. Analysis of the capabilities with filtering technique
 - (a) Filtering technique
 - (b) Results for three-dimensional case: $Re = 300$

Motivations

- Low-order models gave satisfactory prediction results for laminar 2D flows around bluff bodies and, in particular, for the configuration considered in this work. (Galletti *et al.*, JFM, 2004)
- Typical control tools cannot be applied to Navier-Stokes equations (high number of degrees of freedom in their discretization)
- Compute control laws by Reduced Order Models
- State estimation: recover the entire flow field from a limited number of flow measurements

Low-order model construction

- Discrete instantaneous velocity expanded in terms of empirical eigenmodes:

$$\mathbf{u}(\mathbf{x}, t) = \bar{\mathbf{u}}(\mathbf{x}) + \mathbf{c}(t)\mathbf{u}_c(\mathbf{x}) + \sum_{n=1}^{N_r} a_n(t)\phi_n(\mathbf{x})$$

where $\mathbf{c}(t)$ is the feedback control law and $\bar{\mathbf{u}}(\mathbf{x})$ and $\mathbf{u}_c(\mathbf{x})$ are reference velocity fields and chosen such that the snapshots are equal to zero at inflow, outflow and jet boundaries.

- Eigenmodes $\phi_n(x)$ are found by proper orthogonal decomposition (POD) using the “**snapshots method**” of Sirovich (1987).
- Limited number of POD modes, N_r , is used in the representation of velocity fields (snapshots) —→ they are the modes giving the main contribution to the flow energy.

Low-order model construction

- Galerkin projection of the Navier-Stokes equations over the retained POD modes leading to the low-order model:

$$\begin{aligned}\dot{a}_r(t) &= A_r + C_{kr}a_k(t) - B_{ksr}a_k(t)a_s(t) - E_r\dot{c}(t) - F_rc^2(t) + [G_r - H_{kr}a_k(t)]c(t) \\ a_r(0) &= (\mathbf{u}(\mathbf{x}, 0) - \bar{\mathbf{u}}(\mathbf{x}) - \mathbf{c}(0)\mathbf{u}_c(\mathbf{x}), \phi_r)\end{aligned}$$

Low-order model construction

- Galerkin projection of the Navier-Stokes equations over the retained POD modes leading to the low-order model:

$$\begin{aligned}\dot{a}_r(t) &= A_r + C_{kr}a_k(t) - B_{ksr}a_k(t)a_s(t) - E_r\dot{c}(t) - F_rc^2(t) + [G_r - H_{kr}a_k(t)]c(t) \\ a_r(0) &= (\mathbf{u}(\mathbf{x}, 0) - \bar{\mathbf{u}}(\mathbf{x}) - \mathbf{c}(0)\mathbf{u}_c(\mathbf{x}), \phi_r)\end{aligned}$$

- Coefficient B_{ksr} derives directly from the Galerkin projection of the non-linear terms in the Navier-Stokes equations

Low-order model construction

- Galerkin projection of the Navier-Stokes equations over the retained POD modes leading to the low-order model:

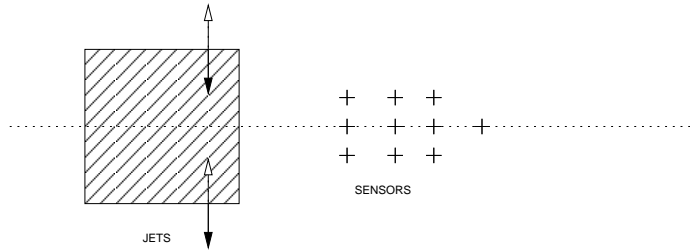
$$\begin{aligned}\dot{a}_r(t) &= A_r + C_{kr}a_k(t) - B_{ksr}a_k(t)a_s(t) - E_r\dot{c}(t) - F_rc^2(t) + [G_r - H_{kr}a_k(t)]c(t) \\ a_r(0) &= (\mathbf{u}(\mathbf{x}, 0) - \bar{\mathbf{u}}(\mathbf{x}) - \mathbf{c}(0)\mathbf{u}_c(\mathbf{x}), \phi_r)\end{aligned}$$

- Coefficient B_{ksr} derives directly from the Galerkin projection of the non-linear terms in the Navier-Stokes equations
- System matrices A , C , E , F , G and H are *calibrated* minimizing

$$\begin{aligned}\mathcal{J} &= \int_0^T \sum_{r=1}^{N_r} \left(\dot{a}_r(t) - \hat{\dot{a}}_r(t) \right)^2 dt + \sum_{r=1}^{N_r} \alpha \left(A_r - \hat{A}_r \right)^2 \\ &\quad + \sum_{r=1}^{N_r} \sum_{k=1}^{N_r} \alpha \left(C_{kr} - \hat{C}_{kr} \right)^2 + \sum_{r=1}^{N_r} \alpha \left(E_r - \hat{E}_r \right)^2 \\ &\quad + \sum_{r=1}^{N_r} \alpha \left(F_r - \hat{F}_r \right)^2 + \sum_{r=1}^{N_r} \alpha \left(G_r - \hat{G}_r \right)^2 \\ &\quad + \sum_{r=1}^{N_r} \sum_{k=1}^{N_r} \alpha \left(H_{kr} - \hat{H}_{kr} \right)^2\end{aligned}$$

where $\alpha \ll 1$.

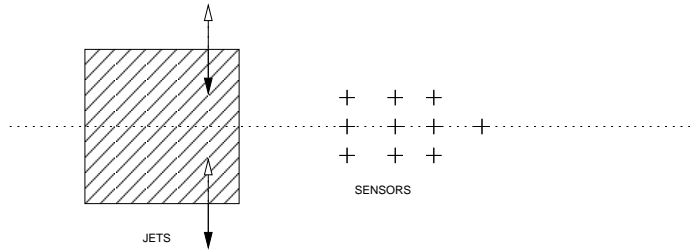
Low-order model construction with feedback actuation



- Control law can be obtained by feedback, using vertical velocity measurements at points \boldsymbol{x}_S in cylinder wake

$$c(t) = K \boldsymbol{v}(t, \boldsymbol{x}_S)$$

Low-order model construction with feedback actuation



- Control law can be obtained by feedback, using vertical velocity measurements at points \mathbf{x}_S in cylinder wake

$$c(t) = K\mathbf{v}(t, \mathbf{x}_S)$$

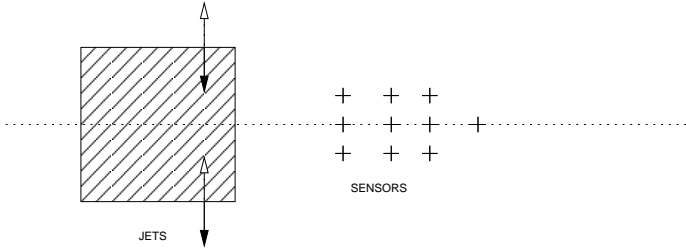
- Developing the velocity at measurements points

$$\mathbf{v}(t, \mathbf{x}_S) = \bar{\mathbf{v}}(\mathbf{x}_S) + c(t)\mathbf{v}_c(\mathbf{x}_s) + \sum_{n=1}^{N_r} a_n(t)\phi_n(\mathbf{x}_s)$$

⇓

$$\mathbf{v}(t, \mathbf{x}_S) = \bar{\mathbf{v}}(\mathbf{x}_S) + K\mathbf{v}(t, \mathbf{x}_S)\mathbf{v}_c(\mathbf{x}_s) + \sum_{n=1}^{N_r} a_n(t)\phi_n(\mathbf{x}_s)$$

Low-order model construction with feedback actuation



- Control law can be obtained by feedback, using vertical velocity measurements at points \mathbf{x}_S in cylinder wake

$$c(t) = K\mathbf{v}(t, \mathbf{x}_S)$$

- Developing the velocity at measurements points

$$\mathbf{v}(t, \mathbf{x}_S) = \bar{\mathbf{v}}(\mathbf{x}_S) + c(t)\mathbf{v}_c(\mathbf{x}_s) + \sum_{n=1}^{N_r} a_n(t)\phi_n(\mathbf{x}_s)$$

⇓

$$\mathbf{v}(t, \mathbf{x}_S) = \bar{\mathbf{v}}(\mathbf{x}_S) + K\mathbf{v}(t, \mathbf{x}_S)\mathbf{v}_c(\mathbf{x}_s) + \sum_{n=1}^{N_r} a_n(t)\phi_n(\mathbf{x}_s)$$

- ⇒ Low-order model with feedback control in compact form:

$$\dot{a}_r(t) = A_r^* + C_{kr}^* a_k(t) - B_{ksr}^* a_k(t) a_s(t)$$

where the matrices A_r^* , B_{ksr}^* and C_{kr}^* are functions of K , $\bar{\mathbf{v}}(\mathbf{x}_S)$, $\mathbf{v}_c(\mathbf{x}_s)$ and $\phi_n(\mathbf{x}_s)$.

Non-linear observer

- Galerkin representation of the velocity field $\mathbf{u}(\mathbf{x}, t)$ in terms of N_r empirical eigenfunctions, $\Phi^i(\mathbf{x})$, obtained by Proper Orthogonal Decomposition (POD)

$$\mathbf{u}(\mathbf{x}, t) = \bar{\mathbf{u}}(\mathbf{x}) + \mathbf{c}(t)\mathbf{u}_c(\mathbf{x}) + \sum_{i=1}^{N_r} a_i(t)\Phi^i(\mathbf{x})$$

Non-linear observer

- Galerkin representation of the velocity field $\mathbf{u}(\mathbf{x}, t)$ in terms of N_r empirical eigenfunctions, $\Phi^i(\mathbf{x})$, obtained by Proper Orthogonal Decomposition (POD)

$$\mathbf{u}(\mathbf{x}, t) = \bar{\mathbf{u}}(\mathbf{x}) + \mathbf{c}(t)\mathbf{u}_c(\mathbf{x}) + \sum_{i=1}^{N_r} a_i(t)\Phi^i(\mathbf{x})$$

- Two simple approaches to estimate coefficients $a_i(t)$:

Non-linear observer

- Galerkin representation of the velocity field $\mathbf{u}(\mathbf{x}, t)$ in terms of N_r empirical eigenfunctions, $\Phi^i(\mathbf{x})$, obtained by Proper Orthogonal Decomposition (POD)

$$\mathbf{u}(\mathbf{x}, t) = \bar{\mathbf{u}}(\mathbf{x}) + \mathbf{c}(t)\mathbf{u}_c(\mathbf{x}) + \sum_{i=1}^{N_r} a_i(t)\Phi^i(\mathbf{x})$$

- Two simple approaches to estimate coefficients $a_i(t)$:
 1. LSQ \Rightarrow approximate flow measurements in a least square sense
(Galletti *et al.* (2004), Venturi & Karniadakis (2004) and Willcox (2006))

$$a_j(\tau) = \sum_{k=1}^{N_s} \Upsilon_{kj}(\Phi(\mathbf{x})) f_k(\mathbf{u}(\mathbf{x}, \tau))$$

Non-linear observer

- Galerkin representation of the velocity field $\mathbf{u}(\mathbf{x}, t)$ in terms of N_r empirical eigenfunctions, $\Phi^i(\mathbf{x})$, obtained by Proper Orthogonal Decomposition (POD)

$$\mathbf{u}(\mathbf{x}, t) = \bar{\mathbf{u}}(\mathbf{x}) + \mathbf{c}(t)\mathbf{u}_c(\mathbf{x}) + \sum_{i=1}^{N_r} a_i(t)\Phi^i(\mathbf{x})$$

- Two simple approaches to estimate coefficients $a_i(t)$:
 1. LSQ \Rightarrow approximate flow measurements in a least square sense
(Galletti *et al.* (2004), Venturi & Karniadakis (2004) and Willcox (2006))
$$a_j(\tau) = \sum_{k=1}^{N_s} \Upsilon_{kj}(\Phi(\mathbf{x})) f_k(\mathbf{u}(\mathbf{x}, \tau))$$
 2. LSE \Rightarrow assume that a linear correlation exists between the flow measurements and the value of the POD modal coefficients
$$a_j(\tau) = \sum_{k=1}^{N_s} \Lambda_{kj}(\hat{a}_j, \hat{f}_k) f_k(\mathbf{u}(\mathbf{x}, \tau))$$

Non-linear observer

- Galerkin representation of the velocity field $\mathbf{u}(\mathbf{x}, t)$ in terms of N_r empirical eigenfunctions, $\Phi^i(\mathbf{x})$, obtained by Proper Orthogonal Decomposition (POD)

$$\mathbf{u}(\mathbf{x}, t) = \bar{\mathbf{u}}(\mathbf{x}) + \mathbf{c}(t)\mathbf{u}_c(\mathbf{x}) + \sum_{i=1}^{N_r} a_i(t)\Phi^i(\mathbf{x})$$

- Two simple approaches to estimate coefficients $a_i(t)$:
 1. LSQ \Rightarrow approximate flow measurements in a least square sense
(Galletti *et al.* (2004), Venturi & Karniadakis (2004) and Willcox (2006))
$$a_j(\tau) = \sum_{k=1}^{N_s} \Upsilon_{kj}(\Phi(\mathbf{x})) f_k(\mathbf{u}(\mathbf{x}, \tau))$$
 2. LSE \Rightarrow assume that a linear correlation exists between the flow measurements and the value of the POD modal coefficients

$$a_j(\tau) = \sum_{k=1}^{N_s} \Lambda_{kj}(\hat{a}_j, \hat{f}_k) f_k(\mathbf{u}(\mathbf{x}, \tau))$$

- Problems with linear estimation (LSQ and LSE) when 3D flows with complicated unsteady patterns are considered

Non-linear observer

- Galerkin representation of the velocity field $\mathbf{u}(\mathbf{x}, t)$ in terms of N_r empirical eigenfunctions, $\Phi^i(\mathbf{x})$, obtained by Proper Orthogonal Decomposition (POD)

$$\mathbf{u}(\mathbf{x}, t) = \bar{\mathbf{u}}(\mathbf{x}) + \mathbf{c}(t)\mathbf{u}_c(\mathbf{x}) + \sum_{i=1}^{N_r} a_i(t)\Phi^i(\mathbf{x})$$

- Two simple approaches to estimate coefficients $a_i(t)$:
 1. LSQ \Rightarrow approximate flow measurements in a least square sense
(Galletti *et al.* (2004), Venturi & Karniadakis (2004) and Willcox (2006))
 2. LSE \Rightarrow assume that a linear correlation exists between the flow measurements and the value of the POD modal coefficients

$$a_j(\tau) = \sum_{k=1}^{N_s} \Upsilon_{kj} (\Phi(\mathbf{x})) f_k (\mathbf{u}(\mathbf{x}, \tau))$$

$$a_j(\tau) = \sum_{k=1}^{N_s} \Lambda_{kj} (\hat{a}_j, \hat{f}_k) f_k (\mathbf{u}(\mathbf{x}, \tau))$$

- Problems with linear estimation (LSQ and LSE) when 3D flows with complicated unsteady patterns are considered
- Contributions in literature aimed to effective sensor placement and extensions of LSE \Rightarrow QSE (Schmit & Glauser (2005), Cohen *et al.* (2004), Cohen *et al.* (2006), Willcox (2006))

Non-linear observer

- Minimize the sum of the residuals

- LSQ case \Rightarrow

$$\alpha(t) = \operatorname{argmin}_{\alpha(t)} \sum_{m=1}^{N_m} \left(\sum_{r=1}^{N_r} R_r^2(\alpha(\tau_m)) + \sum_{r=1}^{N_r} (a_r(\tau_m) - \sum_{k=1}^{N_s} \Upsilon_{kr} f_k(\mathbf{u}(\tau_m)))^2 \right)$$

- LSE case \Rightarrow

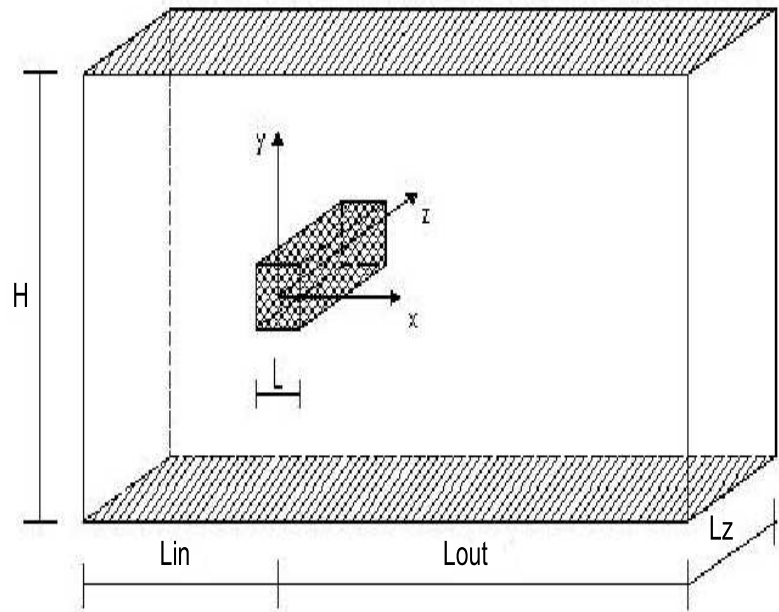
$$\alpha(t) = \operatorname{argmin}_{\alpha(t)} \sum_{m=1}^{N_m} \left(\sum_{r=1}^{N_r} R_r^2(\alpha(\tau_m)) + \sum_{r=1}^{N_r} (a_r(\tau_m) - \sum_{k=1}^{N_s} \Lambda_{kr} f_k(\mathbf{u}(\tau_m)))^2 \right)$$

where $R_r(\alpha(\tau_m))$ is the residual of low-order model

- the method represents a non-linear observer of the flow state (K-LSQ and K-LSE)

DNS : Computational Domain

- Dimensions:
 - $L = 1$
 - $H/L = 8$
 - $L_{in}/L = 12$
 - $L_{out}/L = 20$
 - $L_z/L = 0.6$, 2D simulations
 - $L_z/L = 6$, 3D simulations
- Reynolds numbers based on maximum velocity of incoming profile and “L”



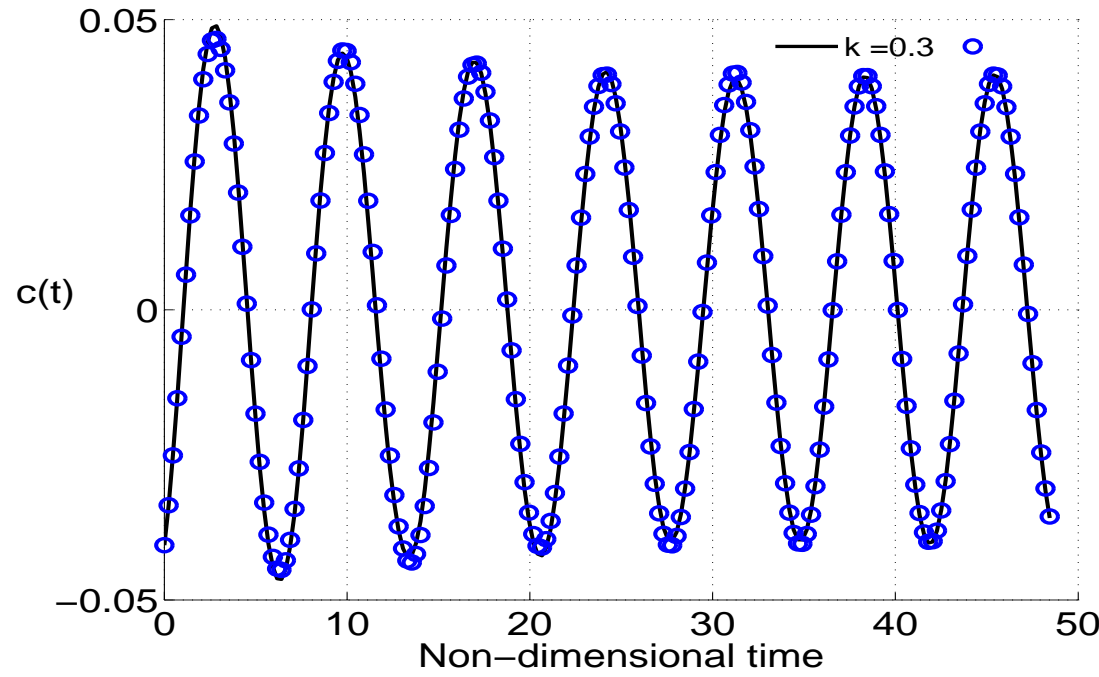
Observer - Results 2D : POD and ROM set-up

- Database

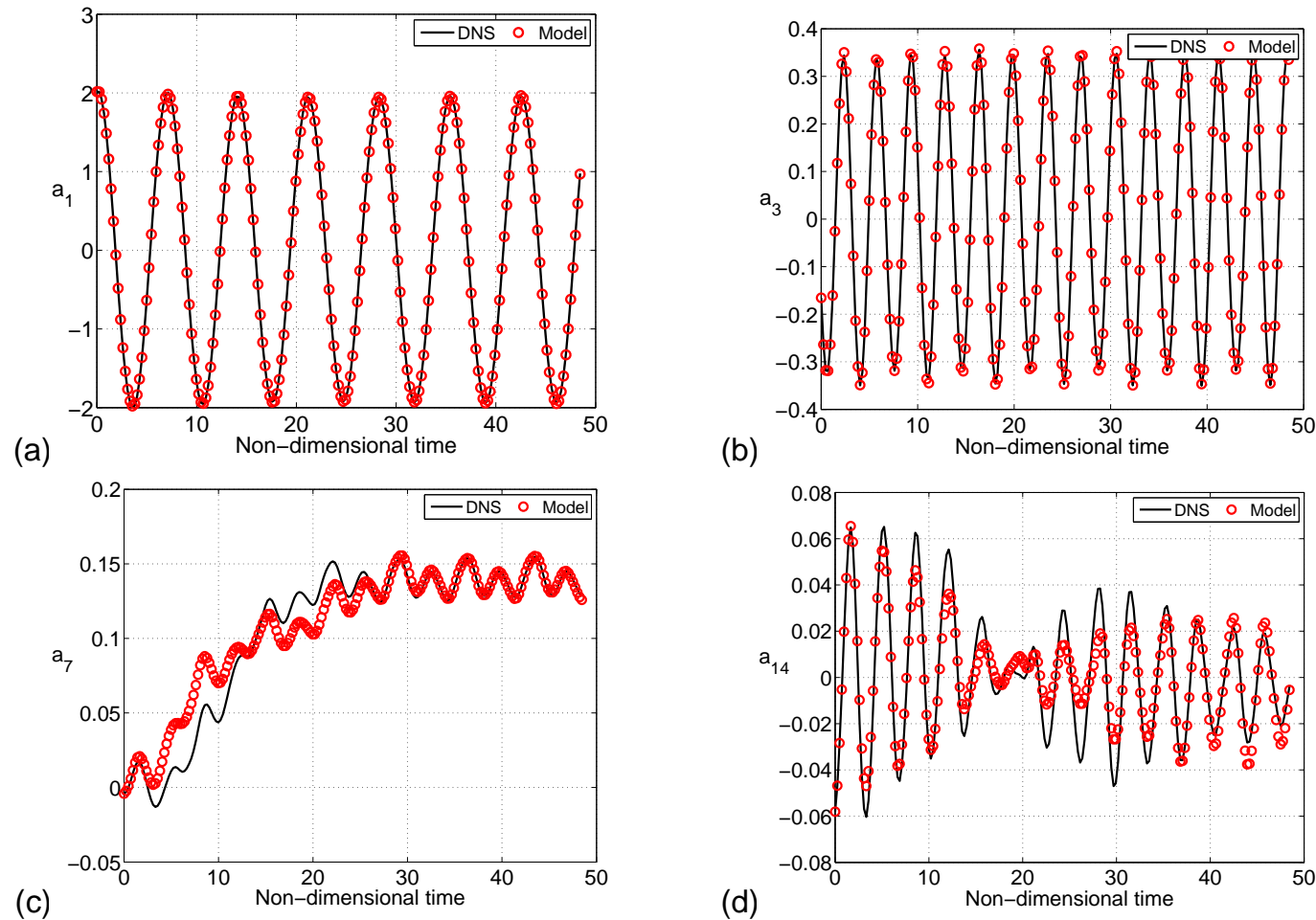
- ≈ 30 snapshots shedding cycle
- $Re = 150 \rightarrow 205$ snapshots
- Feedback gain $k = 0.3$

- Model:

- 205 snapshots from $t = 0.00$ to $t = 48.46 \rightarrow \Delta t = 48.46$
- 20 modes retained $\rightarrow E = 99.7\%$ with a new control law

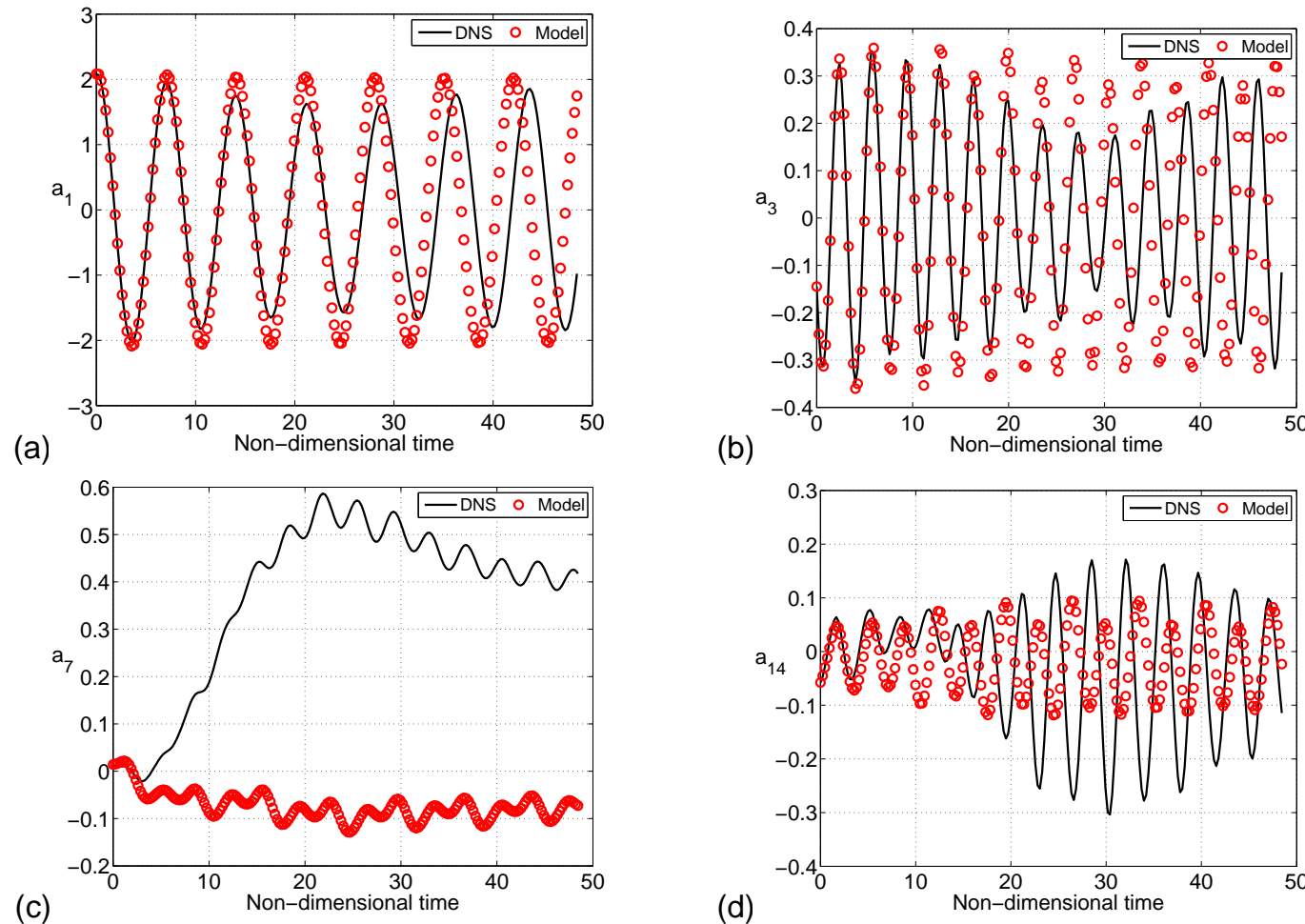


Results 2D: Modal coefficient predictions $k = 0.3$



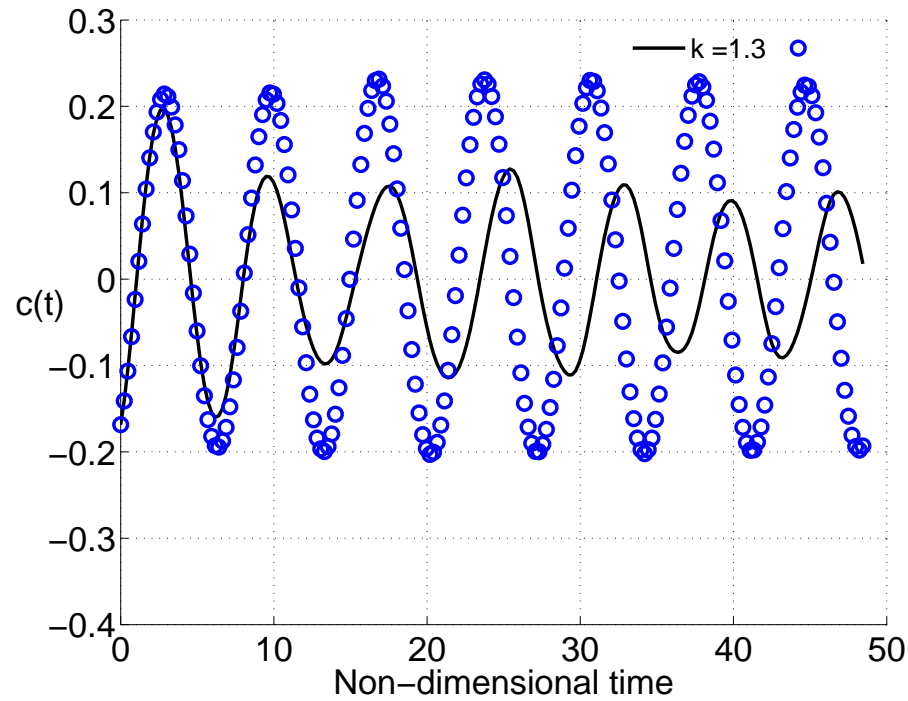
POD modal coefficients a_1, a_3, a_7 and a_{14} . Projection of the fully resolved Navier-Stokes simulations onto POD modes (continuous line) vs. the integration of the dynamical system inside the calibration interval, obtained retaining the first 20 POD modes (circles).

Results 2D: Modal coefficient predictions $k = 1.3$



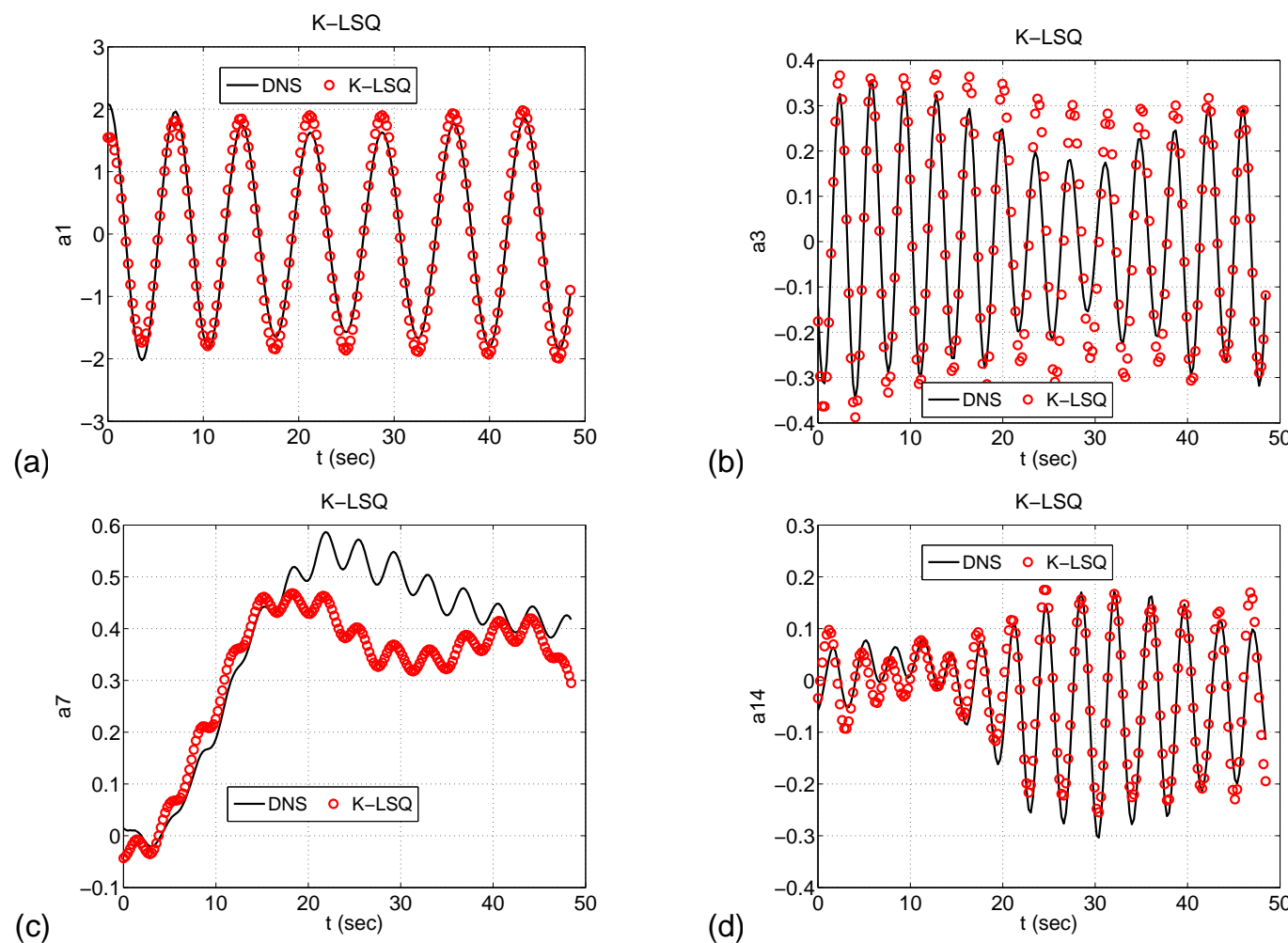
- POD modal coefficients a_1, a_3, a_7 and a_{14} . Projection of the fully resolved Navier-Stokes simulations onto POD modes (continuous line) vs. the integration of the dynamical system with a different feedback gain, obtained retaining the first 20 POD modes (circles).

Results 2D: Control law reconstruction $k = 1.3$



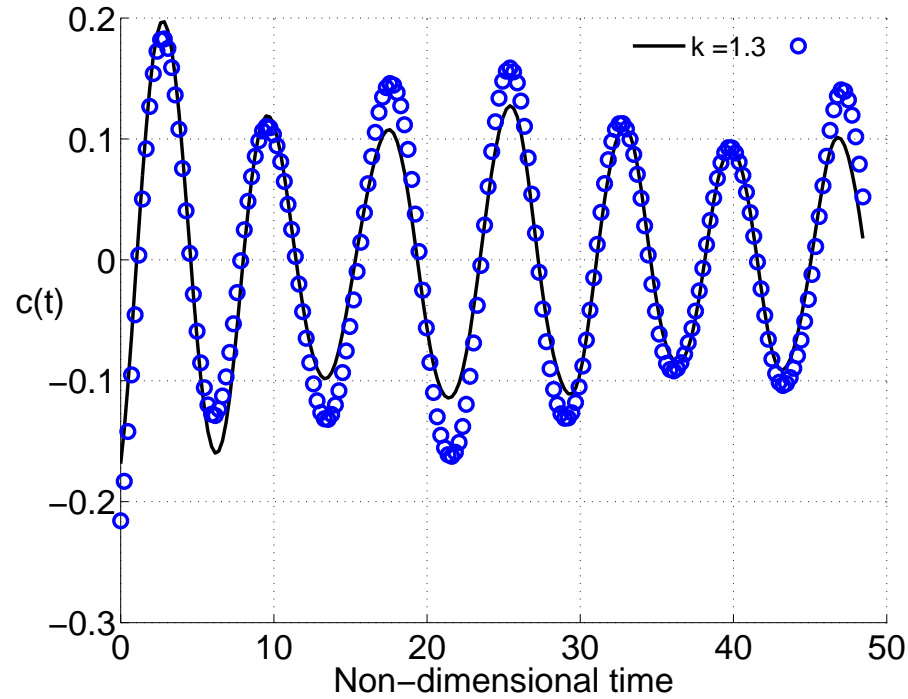
- Projection of the actual control law onto POD modes (continuous line) vs. Reconstructed control law using the integration of the dynamical system with a different feedback gain, obtained retaining the first 20 POD modes (circles).

Results 2D: KLSQ modal coefficient predictions $k = 1.3$



POD modal coefficients a_1, a_3, a_7 and a_{14} . Projection of the fully resolved Navier-Stokes simulations onto POD modes (continuous line) vs. the estimation with the K-LSQ approach (using only six velocity sensors), obtained retaining the first 20 POD modes (circles).

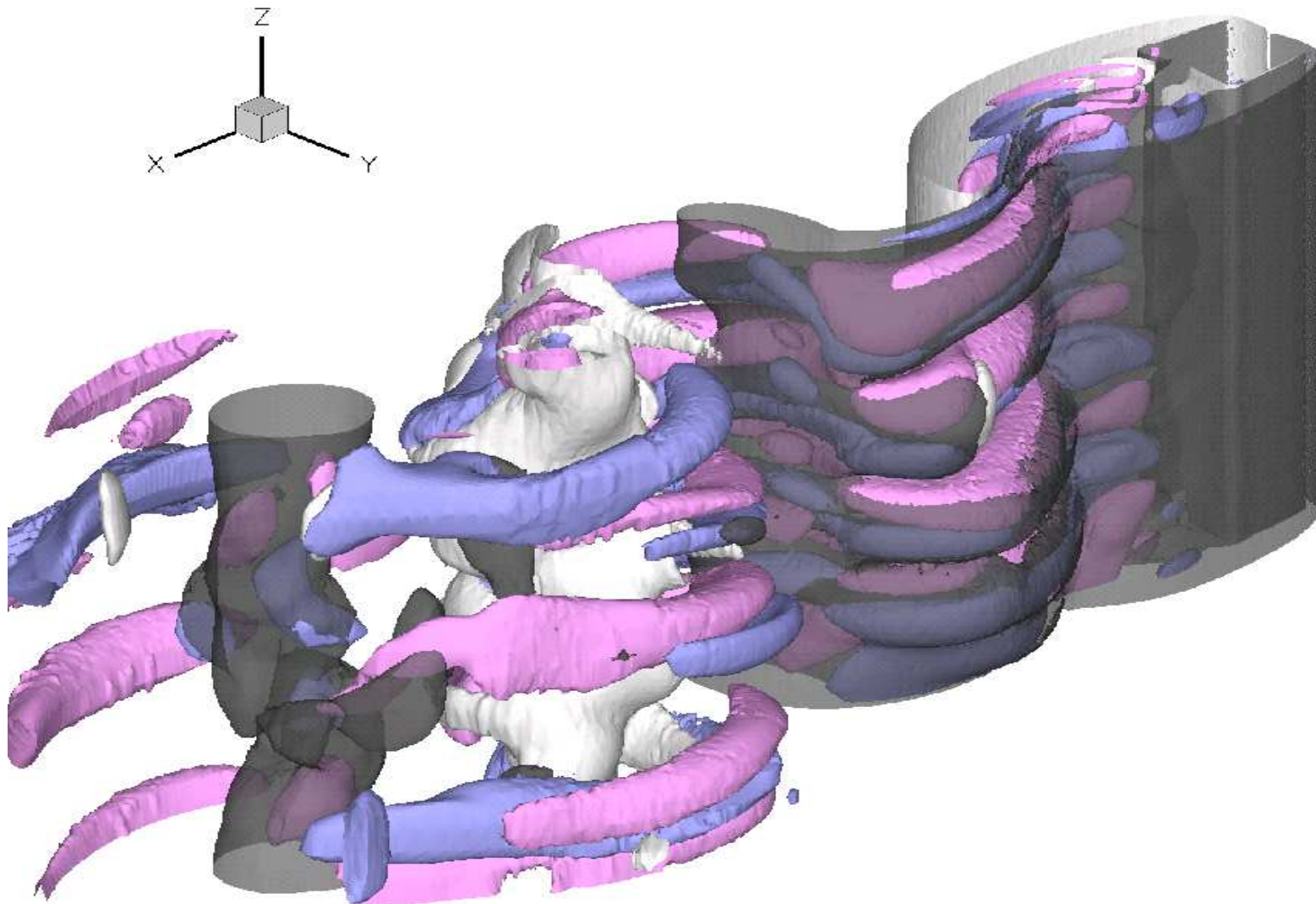
Results 2D: KLSQ reconstruction $k = 1.3$



- Projection of the actual control law onto POD modes (continuous line) vs. Reconstructed control law using the the estimation with the K-LSQ approach (using only six velocity sensors), obtained retaining the first 20 POD modes (circles).

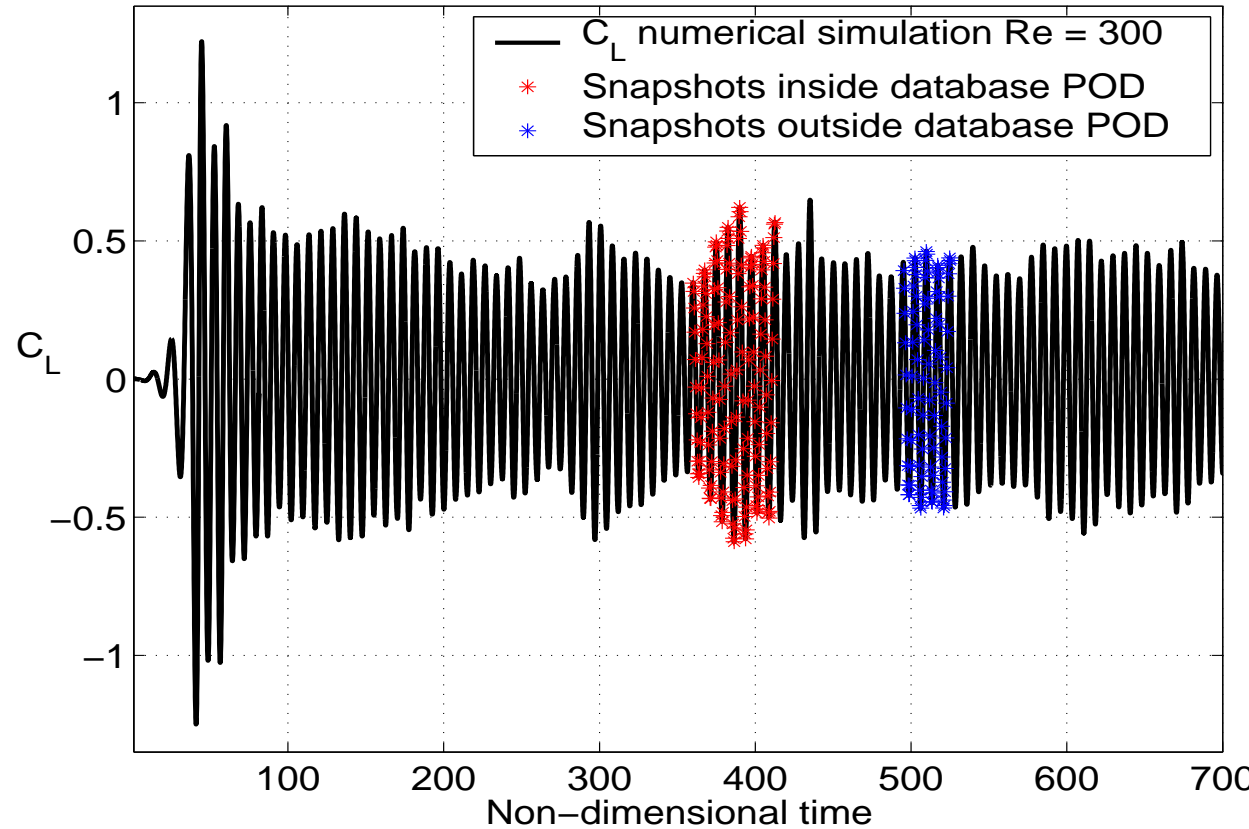
- Actual Flow vs. reconstruction (video)

Considered 3D case for low-order modeling: $Re = 300$

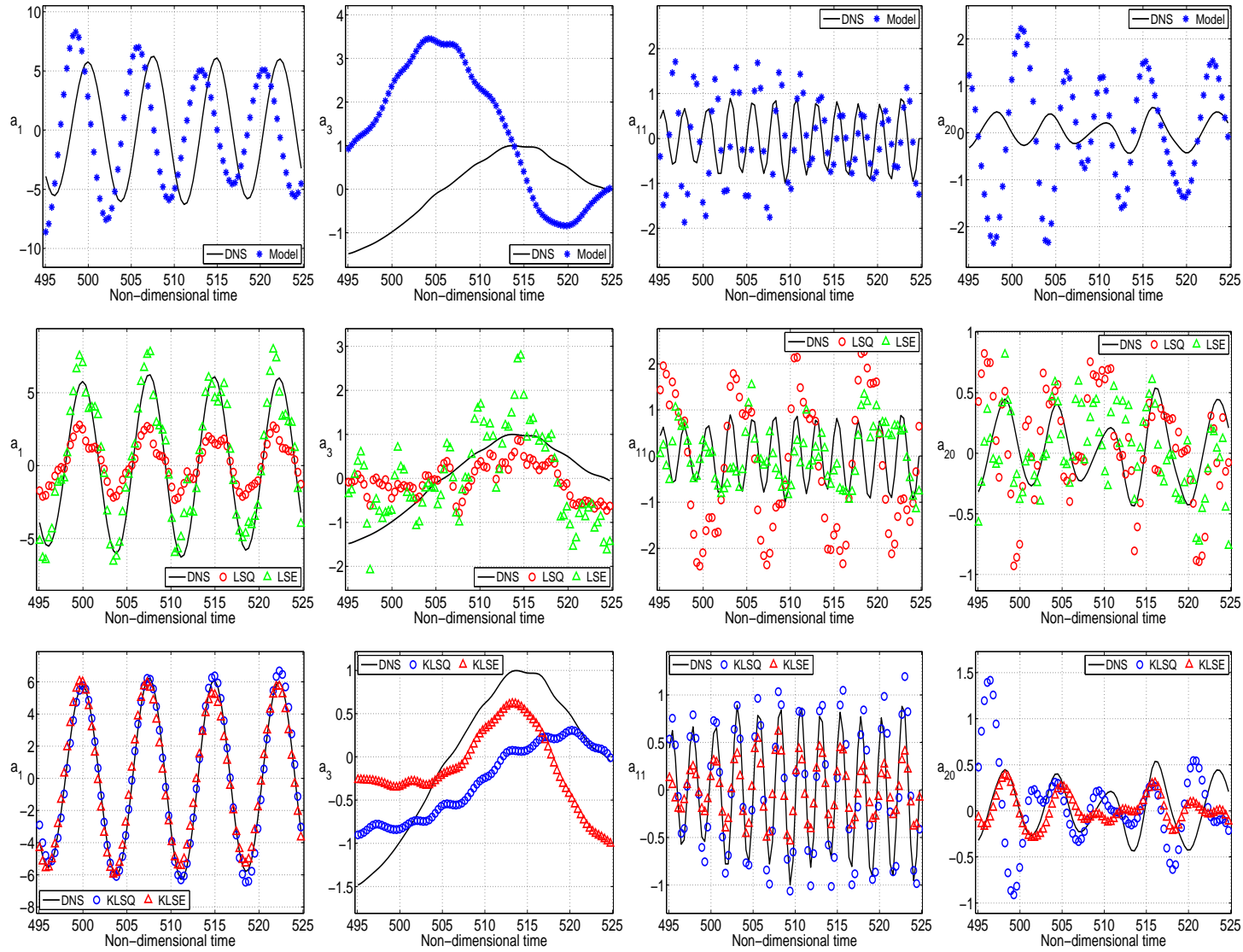


Results 3D : POD and ROM set-up

- Database
 - ≈ 23 snapshots shedding cycle
 - $Re = 300 \rightarrow 1980$ snapshots
- Model:
 - POD : 151 snapshots from $t = 360.23$ to $t = 412.64 \rightarrow \Delta t = 52.41$
 - 20 modes retained $\rightarrow E = 67.6\%$ outside the database



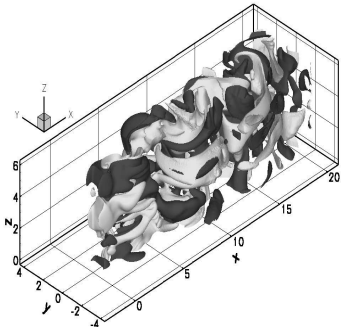
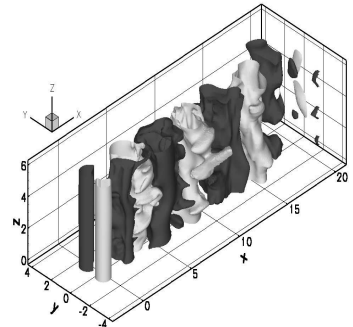
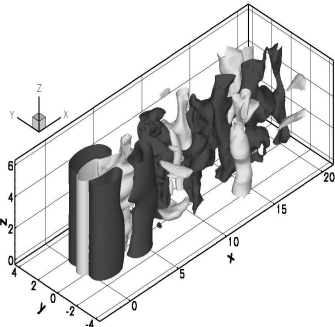
Results 3D: Modal coefficient predictions



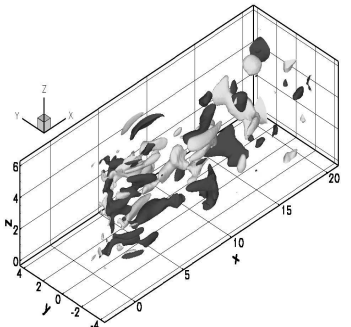
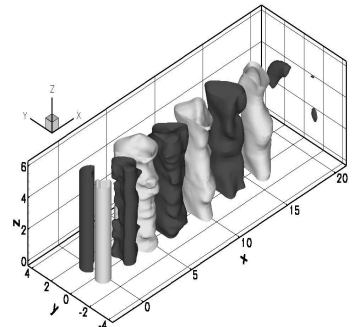
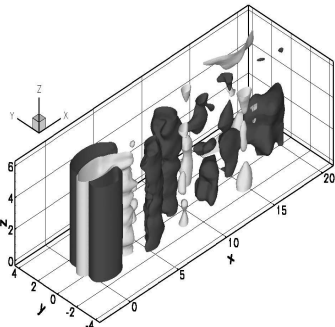
Some representative modal coefficients estimated vs. DNS projections.

1st line : POD-ROM ; 2nd line : LSQ/LSE ; 3rd line : KLSQ/KLSE (24 velocity sensors).

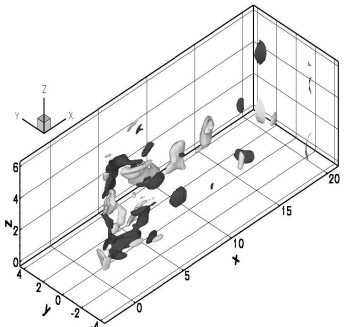
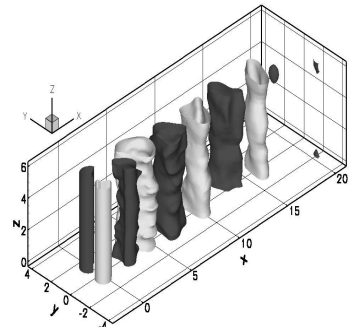
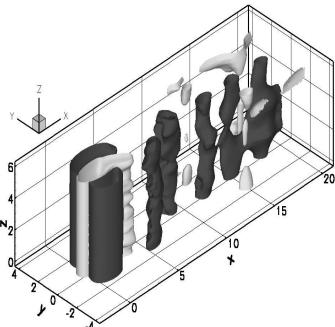
Results 3D : Flow field estimation



(a)



(b)



(c)

Isosurfaces of the velocity components of a snapshot outside the database:



u (left): grey = 0.5
dark grey = 1.0



v (center): grey = -0.25
dark grey = 0.25



w (right): grey = -0.075
dark grey = 0.075



(a) actual snapshot ($t = 426.6$), (b)
snapshot projected on the retained POD
modes,(c) reconstructed snapshot using
the K-LSE technique



Actual Flow vs. Reconstruction (video)

Filtering Technique

- Major limitation is the ability of the POD modes to adequately represent the flow field.
- Filtering technique
 - Space average filter:

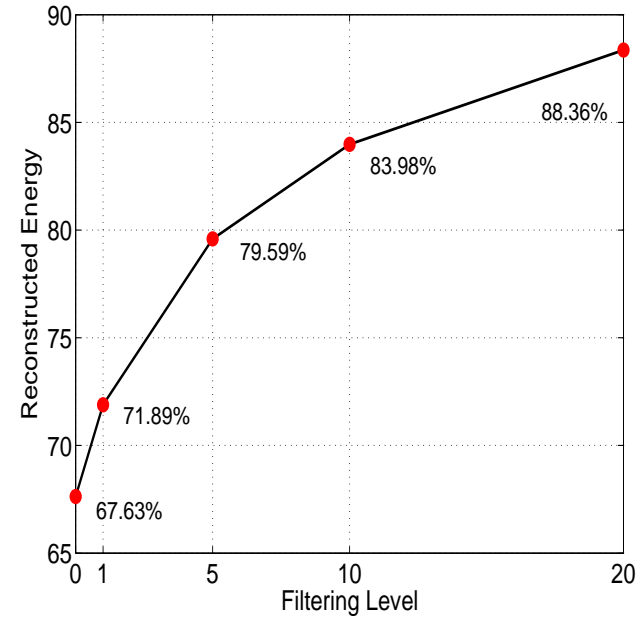
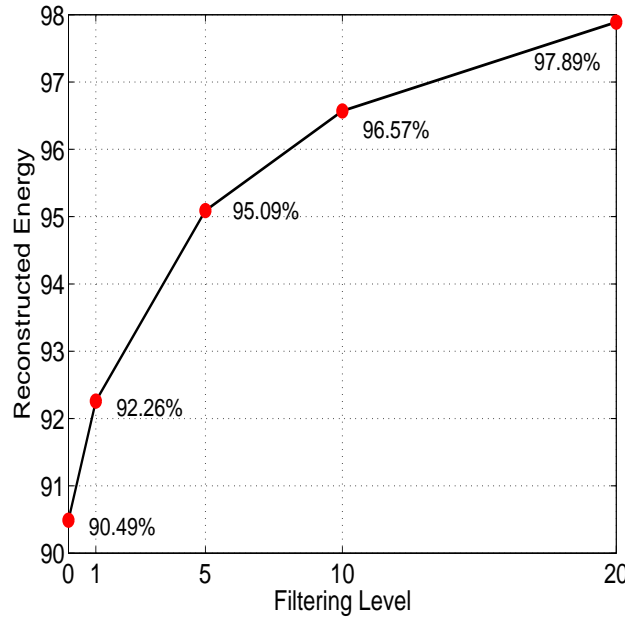
$$\boldsymbol{u}^*(\boldsymbol{x}_j, t) = \frac{\sum_{p \in I_j} V(C_p) \boldsymbol{u}(\boldsymbol{x}_p, t)}{\sum_{p \in I_j} V(C_p)}$$

where I_j is the ensemble of all the vertex of the neighbouring cells of C_j included itself.

Filtering Technique

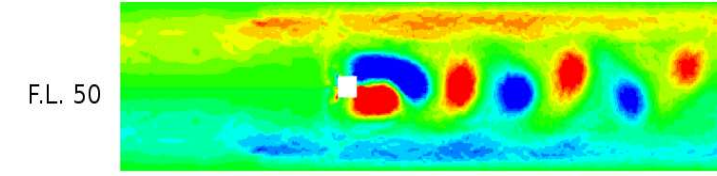
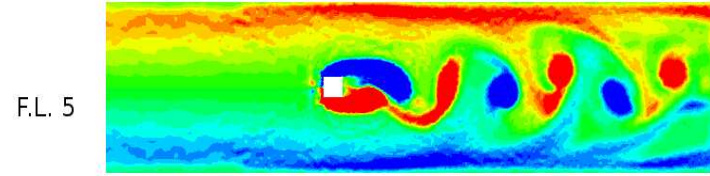
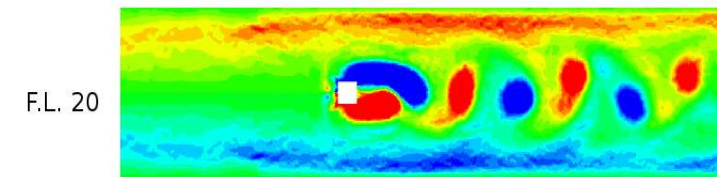
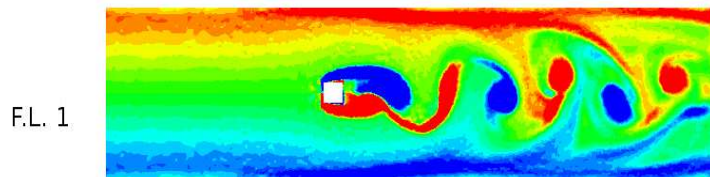
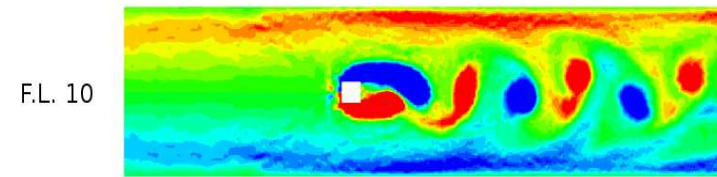
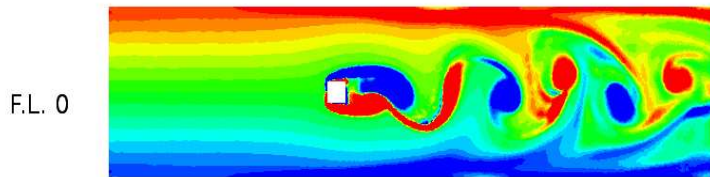


$N_r = 20$ Space Average Filter - Reconstructed energy inside and outside database

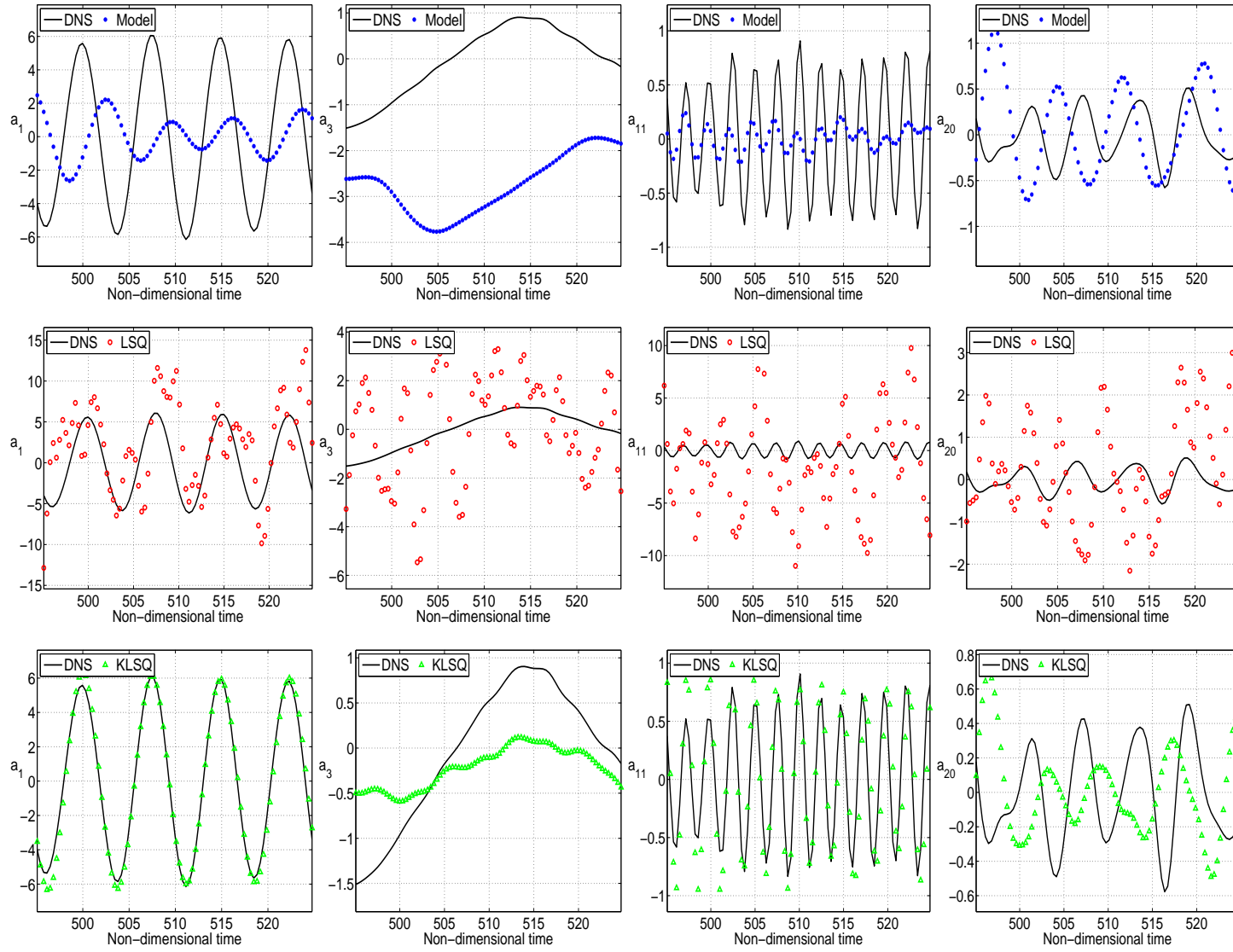


Filtering Technique

- Space Average Filter



Results : Modal coefficients prediction



Some representative modal coefficients estimated vs. DNS projections.

1st line : POD-ROM ; 2nd line : LSQ ; 3rd line : KLSQ (24 velocity sensors - filtering level 5).

Reslts : Flow field estimation

Database		$\overline{e(U')} \%$	$\overline{e(V')} \%$	$\overline{e(W')} \%$	$\overline{e(U)} \%$	$\overline{e(V)} \%$	$\overline{e(W)} \%$
No Filt	min	57.48	43.41	95.57	8.30	40.15	93.47
	KLSQ	64.67	49.77	102.26	9.35	46.02	99.98
Filt 5	min	49.41	33.56	92.37	6.39	30.91	88.77
	KLSQ	58.57	46.23	104.27	7.58	42.57	100.27
Filt 10	min	46.61	29.68	90.83	5.66	27.34	86.23
	KLSQ	54.26	40.01	104.96	6.59	36.83	99.81

- Mean reconstruction error on the U, V, W components for the total and fluctuating field at $Re = 300$: min is the error using the projection of the DNS velocity fields onto 20 POD modes.
- Actual Flow (filtering level 5) vs. Reconstruction (video)**